25th ABCM International Congress of Mechanical Engineering
October 20-25, 2019, Uberlândia, MG, Brazil

# COB-2019-XXXX
# ACTIVE VIBRATION CONTROL APPLIED TO A FLEXIBLE BEAM USING ELECTROMAGNETIC ACTUATORS

**Matheus Rincon Modesto Maroni**
**Willian Faria dos Santos**
**Breno Pagliuse**
**Rodrigo Henriques Lopes da Silva**
**Fabian Andres Lara Molina**
**Edson Hideki Koroishi**

Universidade Tecnológica Federal do Paraná – UTFPR – Campus Cornélio Procópio Av. Alberto Carazzai, 1640 - Centro, Cornélio Procópio - PR, 86300-000
matheusrmaroni@gmail.com
wfsantos92@hotmail.com
pagliuse@alunos.utfpr.edu.br
rodrigolopes@utfpr.edu.br
fabianmolina@utfpr.edu.br
edsonh@utfpr.edu.br

***Abstract.*** *The present contribution is dedicated to active vibration control in a flexible beam using electromagnetic actuators. For this, the structure was built and its parameters were identified. After that, the mathematical modeling of the physical system was done, and from this model, the controller LQR was designed. The methodology was analyzed numerical and experimentally. The numerical control was projected using software MatLab/Simulink and the experimental control was performed in a test bench. Both the numerical and experimental results presented satisfactory results and proved the validity of the proposed methodology.*

***Keywords:*** *Flexible Beam, Active Vibration Control, Electromagnetic Actuator, LQR.*

## 1. INTRODUCTION

Beam elements are of great importance in the civil construction and mechanical fields, as they are commonly used at structures and machines. In particular, due to the great dynamics of operation in the mechanical area, many machines and equipment generate a high level of vibrations, which can often lead to damaging consequences to the structure. Therefore, some techniques were created to control vibrations in structures. Among them, stands out the Passive Control, which is the manipulation of the physical properties of the system, such as mass rigidity and damping in order to minimize vibration and increase system stability (Borges, 2016), and an interesting aspect that justifies the choice of passive control in several applications is that it does not require the use of a complex electronics for its operation (Koroishi, 2013); and the Active Control, which is the most advanced method for vibration attenuation, consisting of sensors, actuators and a control unit. The sensors are responsible for identifying the output variables, the control unit process the information from de sensors, applying the algorithm and the control signals and, finally, the actuators that convert the control signals into the stress actions in the structure (Borges, 2016). Among the active vibration control techniques, Modal Control has been highlighted, mainly because it reduces considerably the computational cost required. This is due to the fact that this technique employs a reduced mathematical model that represents the structure, which has its dynamic behavior satisfactorily described by the use of a limited number of modes that compose its mathematical model (Koroishi, 2013).

The present work is designed to study active vibration control techniques, hereby numerically and experimentally, using electromagnetic actuators at a flexible beam prototype.

## 2. METHODOLOGY

The vibration phenomenon is characterized by a natural oscillatory movement present in structures and equipment. However, when a system exhibits a high level of vibration propagation, it is subject to harmful consequences, such as impairment of its efficiency, resulting in premature wear or even collapse of the structure (Santos, 2018).

In order to solve this problem, vibration control techniques were created. This work aims to study active vibration control techniques in a flexible beam, showed in Fig. 1(a), using electromagnetic actuators, starting by structure assembly, mathematical model, parameters identification, numerical control and finally experimental control.

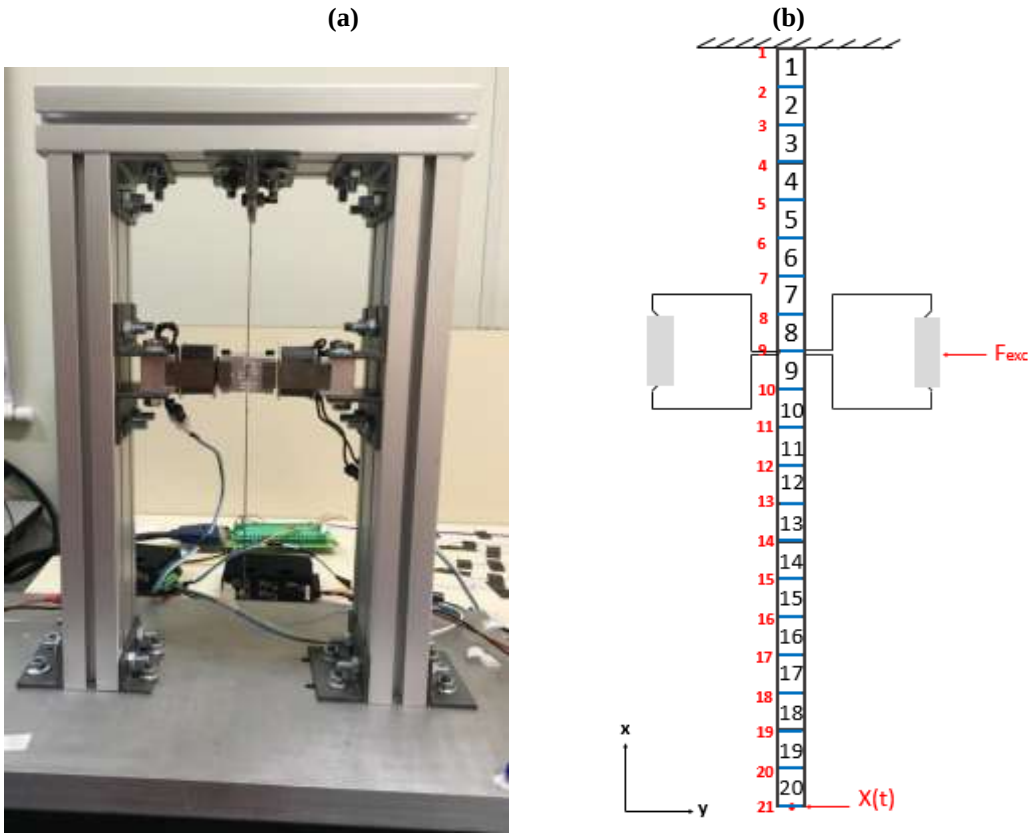


Figure 1. (a) Flexible beam. (b) Model.

## 2.1 System Modeling

The rule dimensions are 300 mm (length), 26.5 mm (width) and 1.0 mm (thickness) and, as shown in the Fig. (1b), the flexible beam has a concentrated mass (where we positioned an "I" pair of the actuators) and is set in a jaw coupled to the upper aluminum profile, supported by 2 columns. It was divided in 20 finite elements, considering two degrees of freedom per node, the first one related to the displacement and the second to rotation, being the first node restricted to these movements due to the crimping. An impulsive force was applied by the actuators themselves at node 9 and the response signal was captured by an accelerometer at node 21. All the 20 discretized elements have 15mm of length and. a pair of actuators positioned in node 9 is a $264{,}07g$ pontual mass.

According to Newton's second law, the motion equation that describes the structure dynamic behavior is represented by Eq. (1)

$$[M]\{\ddot{x}(t)\} + [C_a]\{\dot{x}(t)\} + [K]\{x(t)\} = \{F(t)\} \tag{1}$$

in which $[K]$, $[M]$ e $[C_a]$ are the stiffness, mass and damping elementary matrices respectively, $\{x\}$ the displacement vector and $\{F\}$ is the force applied to the structure.

Using the finite element method and the Euler-Bernoulli model for beams, the elementary matrices [M], [K], [Ca], according to (Azevedo, 2003) are presented by Eq. (2).

$$[K] = \frac{EI}{L}\begin{bmatrix} 12 & 6L & -12 & 6L \\ 6L & 4L^2 & -6L & 2L^2 \\ -12 & -6L & 12 & -6L \\ 6L & 2L^2 & -6L & 4L^2 \end{bmatrix}$$

$$[M] = \frac{\rho SL}{420}\begin{bmatrix} 156 & 22L & 54 & -13L \\ 22L & 4L^2 & 13L & -3L^2 \\ 54 & 13L & 156 & -22L \\ -13L & -3L^2 & -22L & 4L^2 \end{bmatrix} \quad (2)$$

$$[C_a] = \alpha[M] + \beta[K]$$

The matrices [*K*] and [*M* ] depend only on the elastic modulus *E*, the inertia moment *I*, the specific mass ρ, the cross section *S* and the length *L*, while $[C_a]$ also depends on α and β, which are real scalars, and correspond to constants of mass and rigidity proportionality, respectively (Santos, 2018).

The beam model presented by Eq. (1) was written in space states representation, in which, according (Ogata, 2003), it is the form given by Eq. (3).

$$\{\dot{\rho}\} = [A]\{\rho\} + [B_{exc}]\{f\} + [B_{cont}]\{f_{cont}\} \quad (3)$$
$$\{y\} = [C]\{\rho\}$$

Matrix $[A]$ is called dynamic matrix, matrix $[B_{exc}]$ is the input matrix, matrix $[B_{cont}]$ is the control matrix and matrix $[C]$ is the output matrix, while the vector [ρ] corresponds to the state vector.

The parameters *S, L* can be easily measured using a caliper rule, and the parameter *I* can be calculated. However, the parameters *E*, $\rho$, $\alpha$ and $\beta$ cannot be calculated directly. Therefore, it is necessary to use the optimization means to approximate the values of such parameters. The Genetic Algorithm was used to identify parameters.

### 2.2 Genetic Algorithm

A fundamental part for the study of a real system is obtain its mathematical model. Through this model it is possible to evaluate the system dynamic behavior. However, to obtain the mathematical model it is necessary that the system physical parameters are accurately identified.

In this context, one of the ways to obtain these parameters is through the inverse problem methodology, which consists of applying an input to your system and measuring an output (Cavalini, 2015). Knowing the input and its output, you can generate a Frequency Response Function (FRF), and through it use an optimization mean to find the unknown parameters. The present work used the Genetic Algorithm (GA) optimization method.

In a direct problem, system output is determined based on knowing inputs and system parameters. Otherway, in inverse problem the output are known and want to estimate the input or system parameters (Repinaldo, 2018).

Genetic algorithms (GAs) are search methods based on principles of natural selection and genetics (Fraser, 1957; Bremermann, 1958; Holland, 1975). It simulates natural phenomenon, proposing to find the best values that fit the desired curve. GA is a search technique based on natural selection processes for survival through population genetics (Holland, 1992). In order to the GAs begin to evolve, we use selection, crossover, mutation, and substitution steps, where the survival mechanism can be applied to the candidate solutions (Goldberg, 1989)(Haupt e Haupt, 1998).

GAs encode the decision variables of a search problem into finite-length strings of alphabets of certain cardinality. The strings which are candidate solutions to the search problem are referred to as chromosomes, the alphabets are referred to as genes and the values of genes are called alleles. For example, in a problem such as the traveling salesman problem, a chromosome represents a route, and a gene may represent a city. In contrast to traditional optimization techniques, GAs work with coding of parameters, rather than the parameters themselves. (Sastry, 2005).

To evolve good solutions and to implement natural selection, we need a measure for distinguishing good solutions from bad solutions. The measure could be an objective function that is a mathematical model or a computer simulation, or it can be a subjective function where humans choose better solutions over worse ones. In essence, the fitness measure must determine a candidate solution's relative fitness, which will subsequently be used by the GA to guide the evolution of good solutions (Sastry, 2005).

The population size is another GA's important parameter. It affect the scalability and performance of genetic algorithms. The user must choose the best way to set it, once a small population size might lead to premature convergence, and large population size lead to unnecessary expenditure of valuable computational time.

To start to evolve solutions to the search problem, GA follows seven steps. They are Initialization, Evaluation, Selection, Recombination, Mutation, Replacement and the last one is repeat steps 2-6 until a terminating condition is met.

The optimization algorithm GA was executed two hundred time for the following population sizes: 50, 100, 150 and 200. Tab. (1) shows the project space.

Table 1. Parameters range.

| Parameter | Inferior Limit | Superior Limit |
|---|---|---|
| Elastic Modulus [$E$] | $1x10^{12}$ | $1x10^{13}$ |
| Specific Mass[ρ] | $1x10^{3}$ | $1x10^{5}$ |
| Proportionality Constant [α] | 0 | 1 |
| Proportionality Constant [β] | 0 | 1 |

Figure (2) shows the comparison between FRF experimental and identified FRF means for different population sizes, while Fig. (3) shows an approximation in the peaks.

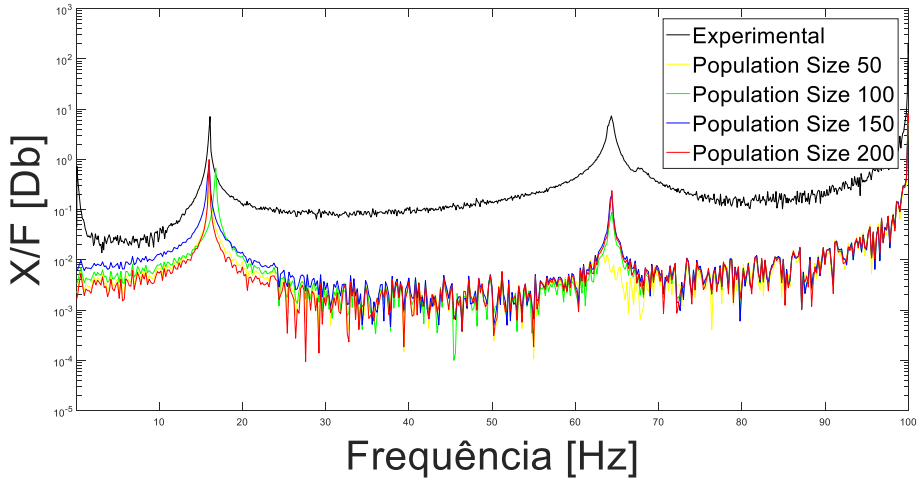


Figure 2. Experimental and identified FRFs.

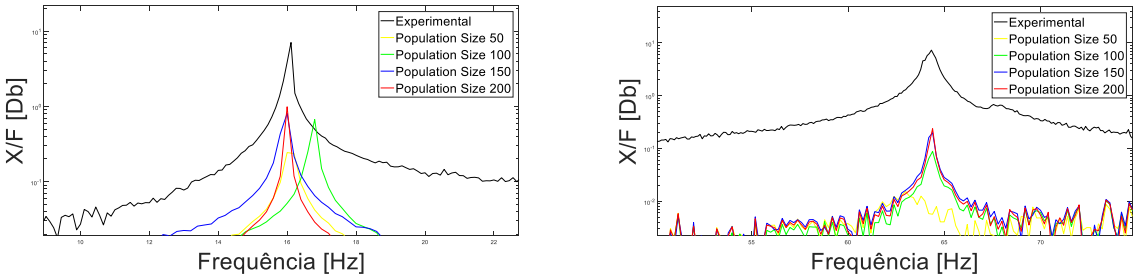


Figure 3. Experimental and identified FRFs peaks.

Table (2) presents the parameters mean and their respective standard deviation.

Table 2. Parameters mean and standard deviation.

| Population Size | Elastic Modulus [$E$] | Specific Mass[ρ] |
|---|---|---|
| 50 | $1.9766x10^{12} \pm 6.99x10^{10}$ | $1.7018x10^{4} \pm 8.99x10^{3}$ |
| 100 | $1.5851x10^{12} \pm 7.49x10^{10}$ | $1.0434x10^{4} \pm 459.91$ |
| 150 | $1.0801x10^{12} \pm 3.81x10^{10}$ | $5.6601x10^{3} \pm 436.47$ |
| 200 | $1.0995x10^{12} \pm 2.91x10^{10}$ | $5.8008x10^{3} \pm 256.20$ |

| Population Size | Proportionality Constant [α] | Proportionality Constant [β] |
|---|---|---|
| 50 | $0.3444 \pm 0.1287$ | $6.1432x10^{-5} \pm 2.8x10^{-5}$ |
| 100 | $0.2188 \pm 0.2208$ | $9.4849x10^{-6} \pm 1.45x10^{-5}$ |
| 150 | $0.3077 \pm 0.3348$ | $1.7718x10^{-6} \pm 3.58x10^{-6}$ |
| 200 | $0.2825 \pm 0.3697$ | $1.9256x10^{-6} \pm 5.96x10^{-6}$ |

As the population increases, the identified curve most closely approximates the experimental curve. Therefore, note that the identified curve that best approached was the red population size 200 curve. However, the standard deviations were relatively high, since not all the curves converged, we chose a curve that best converged among those presented by the optimization with population of 200 and its parameters value are presented by Tab. (3).

Table 3. Identified Parameters.

| Parameter | | | |
|---|---|---|---|
| E $(Pa)$ | $P\ (Kg/m^3)$ | $\alpha$ | $\beta$ |
| $2{,}3971x10^{12}$ | $2{,}2442x10^{4}$ | 0,2964 | $2{,}9873x10^{-5}$ |

### 2.3 Control techniques

Control systems basically deal with the maintenance of quantities such as temperature and pressure at desired operating values or the conduction of a given variable to certain values (Pinheiro, 2009). The control technique obtains data from the stipulate system outputs and the controller makes the necessary decisions with this data, comparing the outputs with a predefined values. Then, the controller sends the necessary commands to the actuator, that adjusts an action to correct the error in order to improve system performance and obtain a variable output as close as desired (Repinaldo, 2018).

The optimum Linear Quadratic Regulator controller is more and more widespread in the literature, due to its performance and ease implementation (PURNAWAN; MARDLIJAH; PURWANTO, 2017). It is widely used in many applications where optimum control is required. The implementation of this control strategy type includes the feedback of the states, which will be weighted in order to minimize a cost function (BURNS, 2001).

Considering a feedback control presented by Eq. (4), the actuators electromagnetic force can be found through the gain controller gain $[K_g]$.

$$\{\dot{x}\} = [A]\{x(t)\} + [B]\{F_{AEM}\}$$
$$\{F_{AEM}\} = -[K_g]\{x(t)\} \quad (4)$$

The controller gain $[K_g]$, according (Ogata, 2003), is determined by minimizing a cost function, given by Eq. (5)

$$J = \int_0^\infty (\{x(t)\}^T [Q]\{x(t)] + \{u(t)\}^T [R]\{u(t)\})dt \quad (5)$$

Which $[Q]$ is a positive definite (or semidefinite positive) or real symmetric Hermitian matrix and [R] is a symmetric positive or real definite Hermitian matrix, with $[R] = [T]^T[T]$, where [T] is a non-singular matrix. Note that the Eq. (5) second term on the right side represents the energy consumption of control signals. The matrices $[Q]$ and $[R]$ determine the relative importance of the error and the consumption of this energy (Ogata, 2003).

Eq. (4) can be rewritten by

$$\{\dot{x}\} = [A]\{x(t)\} - [B][K_g]\{x(t)\} = \big([A] - [B][K_g]\big)\{x(t)\} \quad (6)$$

Considering matrix $\big([A] - [B][K_g]\big)$ is stable or that the eigenvalues $\big([A] - [B][K_g]\big)$ have negative real parts. Substituting Eq. (4). In Eq. (5). Gives Eq. (7).

$$J = \int_0^\infty \{\{x(t)\}^T \Big([Q] + \big[K_g\big]^T [R][G]\Big)\{x(t)\}\}\ dt \quad (7)$$

The Gain matrix $[K_g]$, presented by (Ogata, 2003), is given by Eq. (8).

$$\big[K_g\big] = [R]^{-1}[B]^T[P] \quad (8)$$

In which [P] is a positive definite or symmetric real Hermitian matrix, which can be obtained by solving the reduced matrix equation of Riccati, given by Eq. (9).

$$[A]^T[P] + [P][A] - [P][B][R]^{-1}[B]^T[P]\ + [Q] = 0 \quad (9)$$

### 2.4 Eletromagnetic Actuator

The methodology to obtain the electromagnetic actuator model was previously presented by (Morais, 2013). According him, the magnetic field flux direction is provide due to the winding of the coils in a ferromagnetic core of a sweet iron type, which leads to the losses dispersions reduction. The problem related to the parasitic currents losses (Foucault) is reduced using a core composed by several blades.

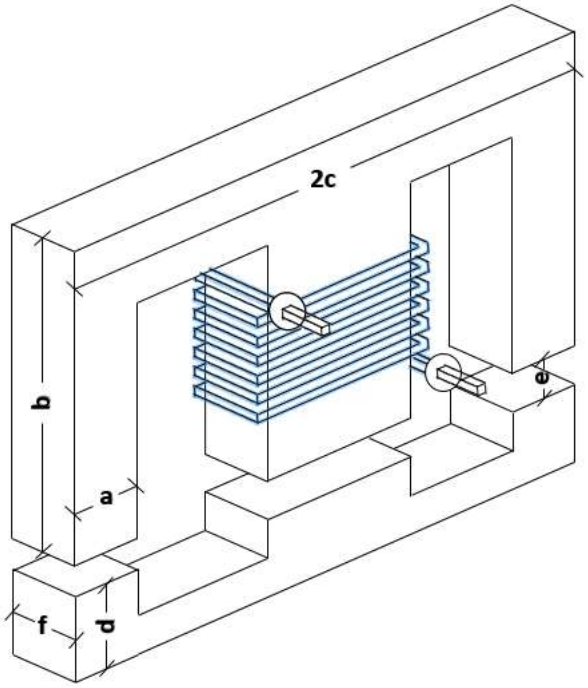


Figure 4. Electromagnetic actuator model (Morais, 2013).

The electromagnetic attraction force between the two ferromagnetic nucleus elements is given by Eq. (10).

$$F_{AEM} = \frac{N^2 I^2 \mu_0 a f}{2\left((e \pm \delta) + \frac{b + c + d - 2a}{\mu_r}\right)^2} \tag{10}$$

where $N$ is number of turns, $I$ the actuator eletrical current, $\mu_0$ the vacuum magnetic permeability, $\mu_r$ the relative permeability, *"e"* the *gap*, $\delta$ the variable that adds to the *gap* to represent the vibration in electromagnetic actuator direction, $a, b, c, d$ and $f$ are constants that represent the actuator geometric parameters. As AEM's just apply attraction force, it should be understood as: the value " $+$ "for $\delta > 0$; and " $-$ " for $\delta < 0$.

Figure (5) shows the real electromagnetic actuator used.

Figure 5. Real electromagnetic actuator.

The AEM's parameters values, extracted by (Koroishi, 2015), is shown in Tab. (4).

Table 4. AEM's parameters.

| Parameter | Value |
|---|---|
| $\mu_0\ (H/m)$ | $4\pi 10^{-7}$ |
| $N\ (espiras)$ | 250 |
| $a\ (mm)$ | 9.5 |
| $b\ (mm)$ | 38 |
| $c\ (mm)$ | 28.5 |
| $d\ (mm)$ | 9.5 |
| $e\ (mm)$ | 1.5 |
| $f\ (mm)$ | 19.5 |

Tab. (4). shows that the electrical current $I$, the displacement $\delta$ and the relative permeability $\mu_r$ are not determined. The electrical current is determined by the control plant, so it is determined according the system request; the displacement, in turn, is a measurable parameter directly on the test bench.

Tab. (5) shows the relative permeability values for each AEM, which were determined experimentally by (Colombo, 2018).

Table 5. AEM's identified values.

| AEM | Median | Average | Mean Deviation |
|---|---|---|---|
| 1 | 727.90 | 662.57 | 9.36% |
| 2 | 397.65 | 468.46 | 8.57% |

An AWG24 standard copper wire is used in the coil winding. This wire characteristics are shown in Tab. (6).

Table 6. AEM's copper coil wire parameters.

| Diameter $(mm)$ | Area$(mm^2)$ | Resistance to 20°C $\left(\frac{Ohm}{m}\right)$ | Maximun Current $(A)$ |
|---|---|---|---|
| 0.511 | 2.205 | 0.0842 | 3.5 |

### 2.5 Test Bench

The experimental control was performed in a test bench. The equipment were assembled according to Fig. (6).

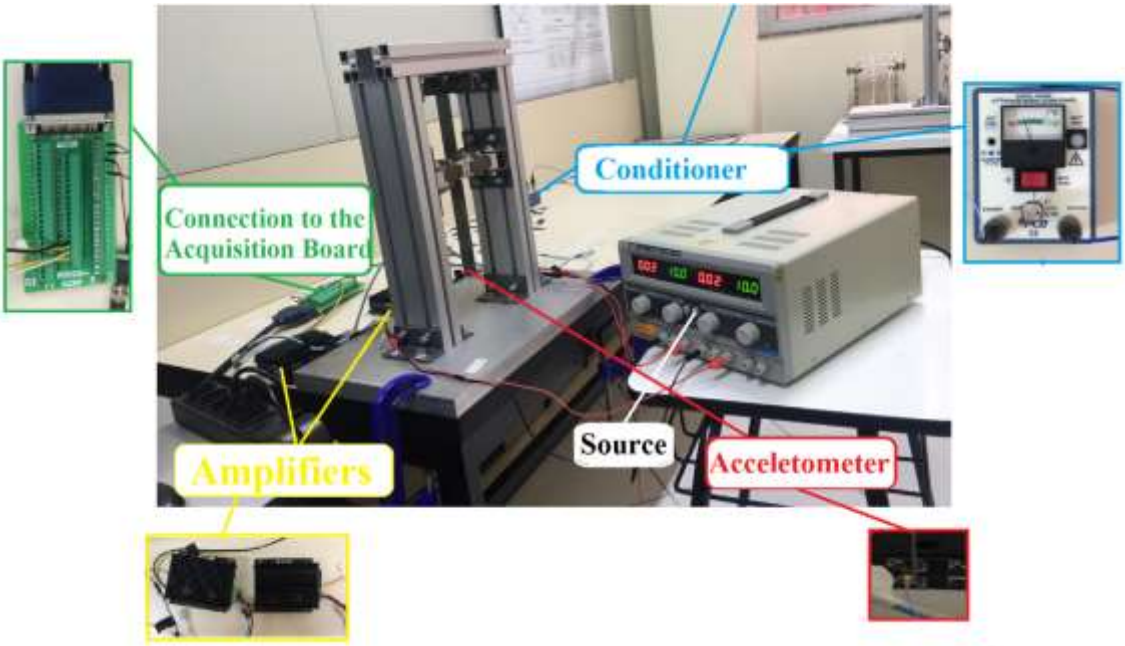


Figure 6. Test bench.

The input force generated by the electromagnetic actuators generates a displacement signal which is measured by the PCB Piezotronics® accelerometer, which has 11.2 $mV/N$ sensibility and the structure natural frequencies are within range of the accelerometer. Then, this signal is transmitted to a signal conditioner in order to improve the measured values accuracy which are conducted to the acquisition board. The conditioner model is PCB Piezotronics® 480E09. The function of amplifiers is converting the board output voltage signal to electric current that will feed the actuators. The model is a Maxon Motor® 4-Q-DC Servo-Amplifier.

With the conditioner sending the signal, the data acquisition is performed through the National Instrument PCI-6221 board, which has 100[Hz] acquisition rate and 10[ms] response time. This board is connected to a desktop computer, and both an analog accelerometer input signal and two voltage outputs that will power the amplifiers are used.

Figure (7) illustrates the schematic experimental control model.

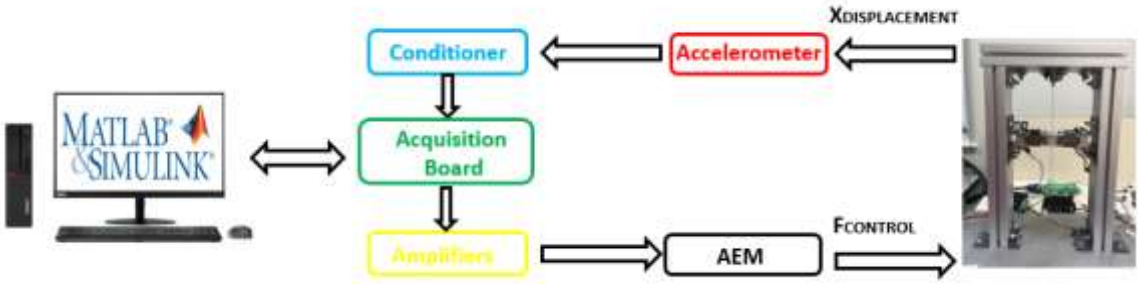


Figure 7. Schematic experimental control model.

## 3. RESULTS AND DISCUSSION

### 3.1 Numerical Control

The numerical control was simulated using the software Matlab/Simulink, and the results are presented in the Figs. (9) to (10).

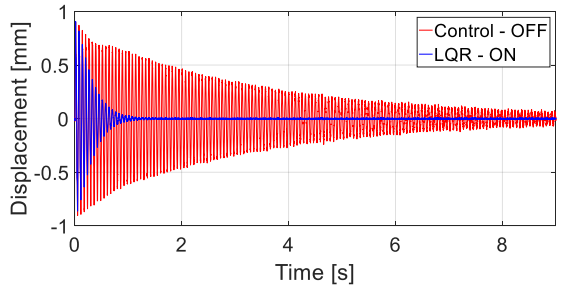


Figure 8. Numerical Displacement.

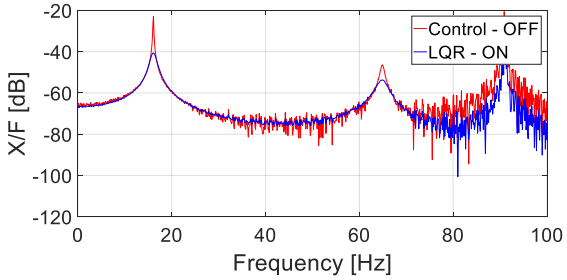


Figure 9. Numerical Frequency Response Function.

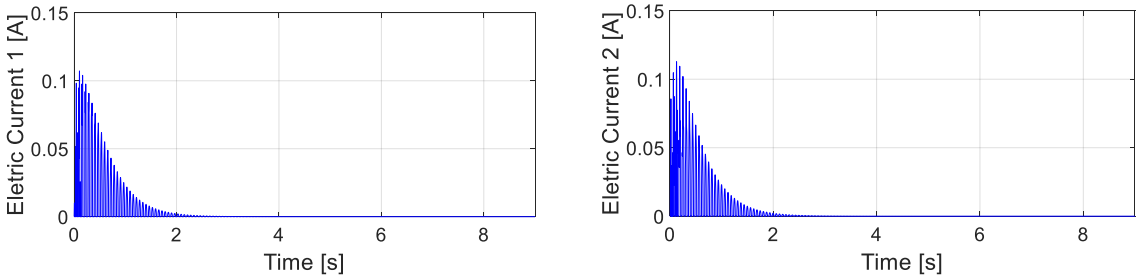


Figure 10. Numerical Electrical Current.

The LQR controller presented a good numerical performance. The accommodation time is about 0.85 s. Analyzing the FRF, the first mode reduction was 17.68 dB and the second mode reduction was 7.45 dB. The maximum electrical current used was 0.1128 [A].

### 3.2 Experimental Control

The experimental control was performed, as showed in Fig. (4), aiming to validate the proposed methodology. The experimental results are presented in the Figs. (11) to (12).

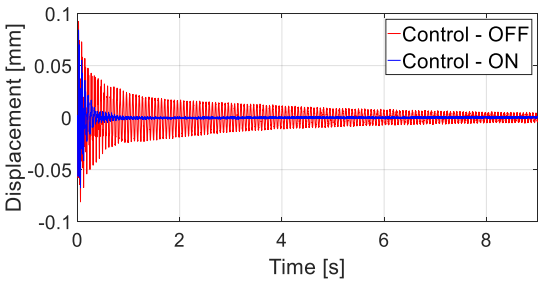


Figure 11. Experimental Displacement.

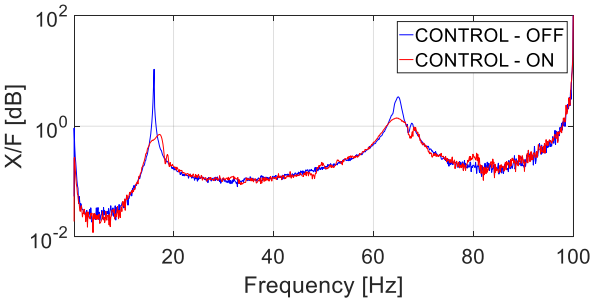


Figure 12. Experimental Frequency Response Function.

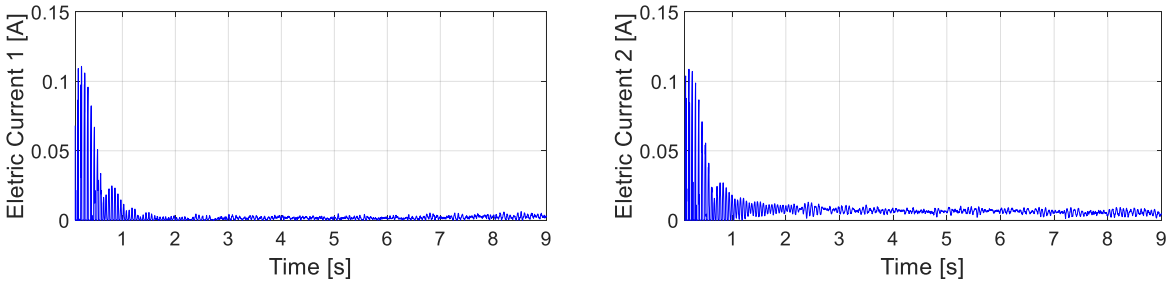


Figure 13. Experimental Electrical Current.

At experimental control, the LQR controller presented an excellent performance, better than numerical. Accommodation time was about 0.5. Analyzing the FRF, the first mode reduction was 9.94 dB and the second mode reduction was 1.97 dB. The maximum electrical current was 0.1108 [A]. It is important to note that shortly small disturbance occurred after the system was controlled, around the time of 1 s, which was caused by the actuator itself, as can be observed by the electric currents that rose slightly above the noise level during that time. This disturbance presents a level slightly higher than the noise and causes this incoherence in the FRF peaks, especially in the first mode.

## 4. CONCLUSION

The present work aimed at the assemble, identification, modeling, numerical and experimental vibration control in a flexible structure that simulates a flexible beam behavior using electromagnetic actuators. Firstly, when the bench was assembled, the structure physical parameters were identified. Then, the dynamic system modeling and the controller design was done, and finally the numerical simulations and experimental control were performed. The LQR controller presented excellent performance both numerically and experimentally.

The negative point to highlight is this small disturbance caused by the actuator that appeared at experimental control, which causes incoherence at the controlled FRF peak. However, in general, it can be concluded that the proposed methodology and the tools used, presented satisfactory results, making possible its use to improve the performance of active vibration control in the flexible structures.

## 5. REFERENCES

Azevedo, A. F. M., 2003, *Método dos Elementos Finitos*. 1ª ed., Faculdade de Engenharia da Universidade de Porto, Portugal.

Borges, A. S.; Koroishi, E. H. ; Oliveira, M. V. F. ; Steffen, Valder. *Controle Robusto em Máquinas Rotativas Utilizando Desigualdades Matriciais Lineares*. In: CONGRESSO NACIONAL DE ENGENHARIA MECÂNICA, 2014, Uberlândia. CONEM, 2014

Burns R. S., 2001, *Advanced Control Engineering*. 1st. ed. London, UK: Butterworth.

Cavalini, Aldemir AP ; Lobato, Fran Sérgio ; Koroishi, Edson Hideki ; STEFFEN Jr, V. . *Model updating of a rotating machine using the self-adaptive differential evolution algorithm.* Inverse Problems in Science & Engineering (Print), v. 1, p. 1-20, 2015

Goldberg, D. E., 1989. *Genetic Algorithms in Search, Optimization and Machine Learning.The University of Alabama*: Society of Automotive Engineers.

Haupt, R. L. & Haupt, S. E., 1998. *Practical Genetic Algorithm*. John Wiley G. Sons Inc

Holland, J. H., 1992. *Adaptation in Natural and Artificial Systems: An Introductory Analysiswith Applications to Biology, Control and Artificial Intelligence*. Cambridge, MA, USA: MITPress

Koroishi, E. H., 2013, *Controle de Vibrações em Máquinas Rotativas utilizando Atuadores Eletromagnéticos*, Tese de Doutorado, Universidade Federal de Uberlândia, Uberlândia – MG.

Koroishi, E.; Lara-Molina, F. ; Borges, A. ; Steffen, V. . Robust control in rotating machinery using linear matrix inequalities. Journal of Vibration and Control, v. 1, p. 1, 2015.

Morais, T S; Hagopian, J. D. ; Steffen Jr, V. ; MAHFOUD, J. . *Modeling and Identification of Electromagnetic Actuator for the Control of Rotating Machinery*. Shock and Vibration, v. 20, p. 171-179

Ogata, K.,2003, *Engenharia de Controle Moderno*, Prentice-Hall do Brasil, São Paulo, Brasil, 788p.

Pinheiro, B., 2009, *Sistema de controle tempo real embarcado para automação de manobra de estacionamento*. Dissertação (Mestrado) - Universidade Federal de Santa Catarina.

Purnawan, H.; Mardlijah; Purwanto, E. B.2017, *Design of linear quadratic regulator (LQR) control system for flight stability of LSU-05*. Journal of Physics: Conference Series, v. 890.

Repinaldo, Silva, C. A. X. ; Santos, W. F. ; Koroishi, E. H. . Identificação de Parâmetros e Controle de um Sistema de Dois Graus de Liberdade. In: X Congresso Nacional de Engenharia Mecânica, 2018, Salvador. Anais do X Congresso Nacional de Engenharia Mecânica, 2018.

Santos, W. F; Silva, C. A. X. ; Repinaldo, J. P. ; KoroishI, E. H. . *Controle ativo de vibrações em uma viga flexível utilizando desigualdades matriciais lineares*. In: VII Simpósio Paranaense de Engenharia Mecânica - SIPEM 2018. 2018, Cornélio Procópio. Anais do VII Simpósio Paranaense de Engenharia Mecânica - SiPEM 2018, 2018.

Sastry, K., Goldberg, D., & Kendall, G. (2005). *Genetic algorithms*. In E. K. Burke & G. Kendall (Eds.), Search methodologies: introductory tutorials in optimisation and decision support techniques.

## 6. ACKNOWLEDGMENT

Thanks to UTFPR, for the support and material that made possible this work accomplishment. This work was carried out with the Conselho Nacional de Desenvolvimento Científico e Tecnológico CNPq - Brasil (Processo 402581/2016-4) support. I thank CNPq, which financied a PIBIC scientific initiation grant.

## 7. RESPONSIBILITY NOTICE

The authors are the only responsible for the printed material included in this paper.